THE WIRE POSITION MONITOR (WPM) AS A SENSOR FOR MECHANICAL VIBRATION FOR THE TTF CRYOMODULES

A. Bosotti, C. Pagani, R. Paparella, P. Pierini, D. Sertore INFN LASA, Milano, Italy
R. Lange, DESY, Hamburg
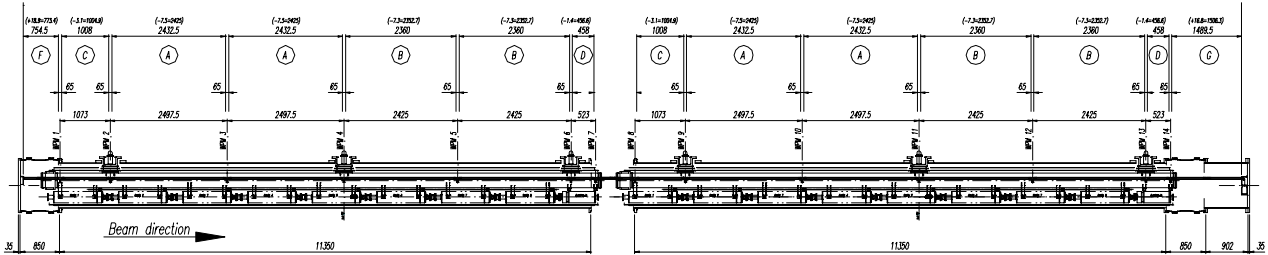R. De Monte, M. Ferianis, ELETTRA, 34012 Trieste Italy

Figure 1: The longitudinal positions of the WPM sensors in cryomodules # 4 and # 5.

Abstract

The WPMs installed on the last two TTF cryomodules can be used as microphonic and sub-microphonic vibration detectors. The spectra taken during a first test using the normal readout electronics, performed using the last four WPMs of the 5th cryomodule, has shown that the system has the necessary sensitivity needed to detect small mechanical vibrations (resolving up to 100 nm) in the 0.01-100 Hz range. The mechanical vibrations can be recovered de-modulating the WPM RF signals, amplitude modulated by the TTF cold mass mechanical vibrations. In this paper we show the potentialities of our system to achieve resolutions in the nanometer range, together with the analysis of vibration spectra of crucial parts of cryomodules 4 and 5 of the TTF.
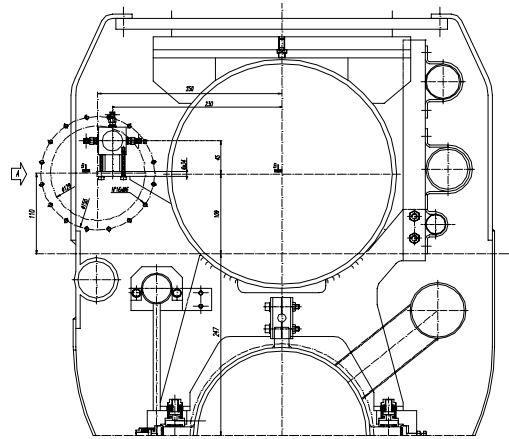
INTRODUCTION

A Wire Position Monitor (WPM) system has been developed for on-line monitoring the cold mass movement and deformation during cooldowns and normal operation. The analysis of the WPM measurements between successive cooldown cycles allows checking the alignment reproducibility. This information contributes to the improvements of the design that brought to the actual generation of cryomodules. Furthermore, together with the cryomodule evolution, the WPM system sustained substantial modifications and simplifications. Starting from two chains of 18 detectors for the first generation of cryomodules, nowadays only a single chain of seven detectors (placed in critical positions: at each end, at the three posts and between the posts) is used, the WPM being now screwed, through a support, to a stainless steel arm which is welded to the gas return pipe (GRP). In Fig. 1 the drawing of the 3rd generation cryomodules # 4 and # 5 connected in chain is shown, together with the longitudinal positions of the monitors. Fig. 2 shows a cross section of the actual 3rd generation cryomodule with the WPM screwed to the supporting arm (middle-left).

Figure 2: Cross section of the TTF cryomodule showing the WPM screwed to its supporting arm.

A WPM is a sort of microstrip four channel directional coupler [1]. A 140 MHz RF signal is applied on a stretched wire placed (nominally) in the center of the monitor bore and is sampled by the four microstrips, leading to the detection of the wire relative position both in the horizontal and in the vertical planes. The de-modulated electrical signals between opposite electrodes are converted in cold mass displacement (horizontal and vertical) via a two dimensional 3rd order polynomial. Moreover this kind of monitor has been proved to be useful as vibration detector [2], and after a successful "evaluation" testing activity, with the acquisition of the vibrations coming from the last four WPMs of the 5th module, the measurement has been extended to all the monitors of the cryomodules #4 and #5. In the following sections we will present, for both cryomodules, the spectra of the vibration noise measured close to the central posts and close to the cryomodule ends. The former positions are where all the cold mass is constrained and consequently the noise immunity is high, while the latter are where the sensibility to the mechanical noise disturbances is higher.

THE WPM AS VIBRATION DETECTOR

The low frequency vibrations of the cold mass are rigidly transfer to the WPM producing an amplitude modulation of the RF signal picked up by the WPM microstrips. So, due to the high broadband characteristics of a stripline detector, the microphonics (and the sub-microphonics) can be recovered de-modulating the microstrip picked up RF signal. For this purpose the WPM control electronics has been upgraded inserting a 4 channel Digital Receiver Board, that recovers the base-band signal like a sort of AM software radio. The de-modulated signals are converted into position via the same two dimension 3rd order polynomial, used to convert electrical signals into WPM displacements. The Digital Receiver board can acquire vibration spectra independently from the WPM normal operation and with different signal sampling rates. The acquisition time is set accordingly to the desired frequency resolution. Another nice feature of the WPMs is that they work in the same way at cold (2 K) and warm (room temperature) conditions. Moreover they are well distributed along the cryomodules, allowing an accurate analysis all along the modules length. A possible limitation of the WPM system to the detection of vibration spectra could be the amplitude of the stretched wire proper oscillations. Using the vibrating string equation (VSE) and inserting our system parameters (the stretched wire is made of CuBe, from Berylco-Cabot BERYLCO 25), we find

$$f_n = \frac{n}{2\ell}\sqrt{\frac{F}{\rho A}} = n \cdot 6.362 \ \text{Hz} \qquad (1)$$

where

- Density (ρ): 8.25 g/cm^3 = 8250 kg/m^3
- Cross Section (A): 0.196 mm^2
- Stretched Wire Length (ℓ) 25.950 m
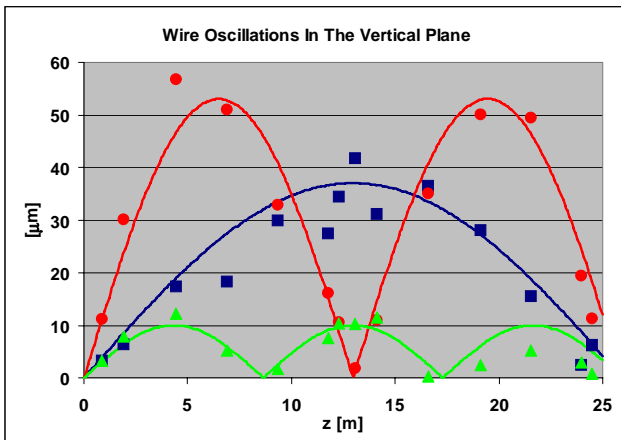- Tensile Strength (F): 18 kgp = 176.58 N

Figure 3: Measured spatial pattern of the stretched wire self oscillation harmonics for the first three harmonics

Being the stretched wire proper frequency in the band of sub-microphonic frequencies, we expect to find it and its harmonics superimposed to the spectra of the cold mass vibrations we want to detect. Nevertheless, being their frequencies well predictable by VSE which completely agrees with the experimental data (Fig. 3), it is rather easy to filter them while processing the data.

SYSTEM DESCRIPTION

The vibration detection system is a super-heterodyne receiver where the base-band demodulation is made digitally [3]. This has two advantages. One is the programmability, which means that new functions and
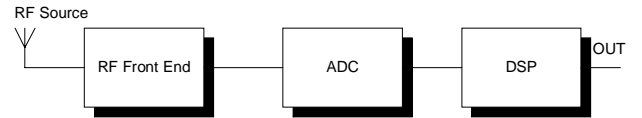

Figure 4: Digital receiver concept

upgrades to the system don't require hardware re-design but only the writing and loading of new software code. The other advantage is the increase in linearity, that in a conventional analog receiver is defined by the most nonlinear element of the processing chain, which is usually the analog demodulator. Digital receiver on the other hand implements digital demodulation, which shifts the source of non-linearity either to the RF front end or the Analog to Digital Converter (ADC). While ADCs offer excellent linearity properties, a careful RF front end design is needed. A block diagram of the system is shown in Fig. 4.

The system is interfaced with the DOOCS-based TTF control system via a VME board computer, and can be remotely controlled. Vibration spectra are locally stored to the VME board computer hard disk, and then transferred through secure FTP protocol, for data analysis. Here follows a short description of the main features of the RF input stage and of the Digital Receiver board.

RF Front End

Two WPM readout electronics boards have been modified inserting RF buffers after their input stages, to work as the RF front end circuitry for the digital receiver.
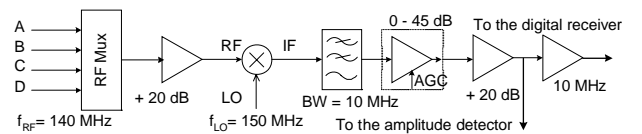

Figure 5: Modified RF input stage with down-converter, AGC and output to digital receiver.

The function of the RF front end is to read the four microstrips of the desired WPM, and to down-convert the RF signal to the 10 MHz IF signal. In Fig. 5 the RF input stage block diagram is shown. The RF signals coming from the monitor are applied to a four channel RF multiplexer, and are switched to a common read out and processing circuitry. The multiplexer is based on HP 5082 pin diodes that ensure very high linearity. The RF 140 MHz signals, after being amplified by 20 dB trough a MAR 6 RF amplifier, are down converted to the 10 MHz

IF frequency signal with a double balanced mixer. The IF signal is applied to an Automatic Gain Amplifier (AGC) module. The gain is set by the control software and its purpose is to minimize non-linearity effects by driving all the active components well below the 1 dB compression point, and to guarantee enough signal amplitude to make the digital receiver work efficiently.

Digital Receiver

The digital receiver board is a Quad Digital Receiver (QDR) module from Instrumentation Technologies [4]. The IF signals from the RF front end enter the QDR, where they are first filtered, and then sampled. The Analog Devices 14 bit AD9644 analog to digital converter is used for the A to D conversion. The AD6644 is designed specifically to address the needs of wideband multichannel receivers and maintains 100 dB dynamic range over the Nyquist band. Typical signal-to-noise ratio is 74 dB. The AD6644 is mounted on a mezzanine board, attached to the main board. A block diagram of the QDR board can be found in Fig. 6.
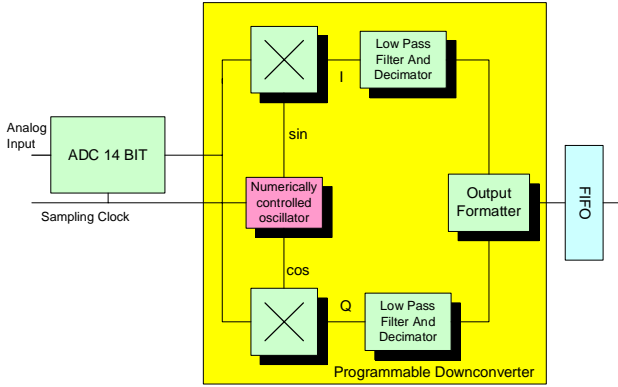

Figure 6: Digital Receiver functional Diagram

The rest of the processing is done in a digital way. The Digital Down-converter (DDC) translates the carrier to base-band and then applies filtering and decimation, gain scaling, re-sampling and Cartesian to polar coordinate conversion. The process of filtering is very important: filtering defines system bandwidth; and decimation, a reduction of the output data rate with respect to the input, significantly reduces the downstream digital signal processing of the DDC.

MICROPHONIC VIBRATIONS ON MODULES # 4 AND # 5

The WPMs of two modules were scanned by the Digital Receiver at 5 kHz sampling frequency with an acquisition time 30 s long. In this way the spectral bandwidth is df ≈ 0.035 Hz. WPMs # 4 (cryomodule # 4) and # 11 (cryomodule # 5) are close to the central posts, where all the cold mass is constrained, while WPMs # 7 and # 14 are at the end of the corresponding cryomodule, in the proximity of the quadrupoles. We will start analyzing the spectra of vibration signal coming from these four monitors, because of their position in crucial points of the cold mass string. The data were taken between 2 and 4 P.M. of Friday 17 June 2005, with the cryomodules cooled down and in stationary condition. The cavities were not excited by the klystrons. The vibration spectra magnitude of the signal measured on the cryomodule # 4 (WPM #4 and #7), in the horizontal and vertical planes respectively, are shown in the Fig. 7 and Fig. 8, while the ones corresponding to the module # 5 (WPM #11 and #14) are shown in Fig. 9 and Fig. 10. The wire proper frequencies have been filtered.
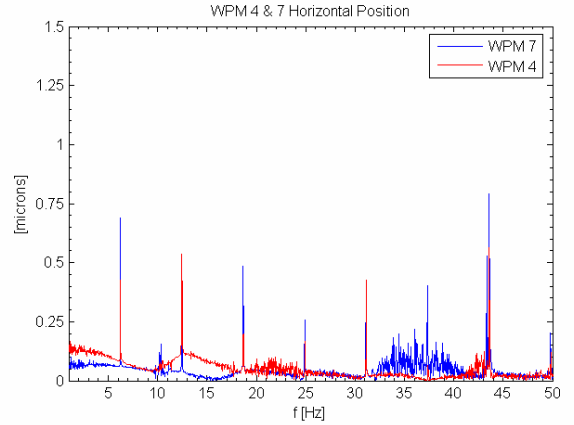

Figure 7: Spectra of cold mass vibrations in the horizontal plane, detected by WPM # 4 and # 7. A residual of wire proper oscillation (after filtering) is still present.
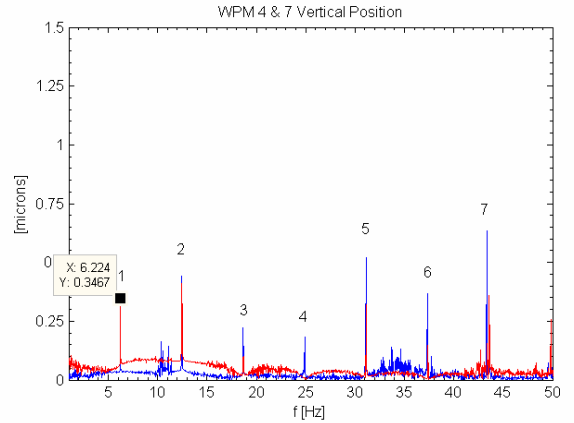

Figure 8: Spectra of cold mass vibrations in the vertical plane, detected by WPM # 4 and # 7. The harmonic number (for the first 7 harmonics) is reported close to each spectral line for the superimposed stretched wire oscillation spectral lines.

Equation (2) has been used to compute the FFT amplitudes for the spectral lines (N = samples number, τ = sampling interval) [5]:

$$G\left(\frac{n}{N\tau}\right) = \frac{2}{N}\sum_{k=0}^{N-1} g(k\tau)\cdot e^{-j\frac{2\pi}{N}nk} \qquad n = 1\ldots\frac{N}{2}-1$$

$$G(0) = \frac{1}{N}\sum_{k=0}^{N-1} g(k\tau) \qquad\qquad n = 0$$

(2)

In Fig. 8 for clearness, the harmonic number of the wire proper oscillation eigenmodes is reported close to each spectral line (up to the 7th harmonic) to ease their identification, in order to avoid confusing them with the cold mass vibration spectral lines.
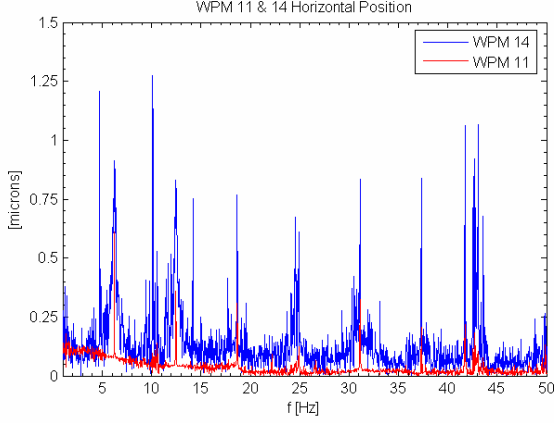

Figure 9: Spectra of cold mass vibrations in the horizontal plane, detected by WPM # 11 and # 14
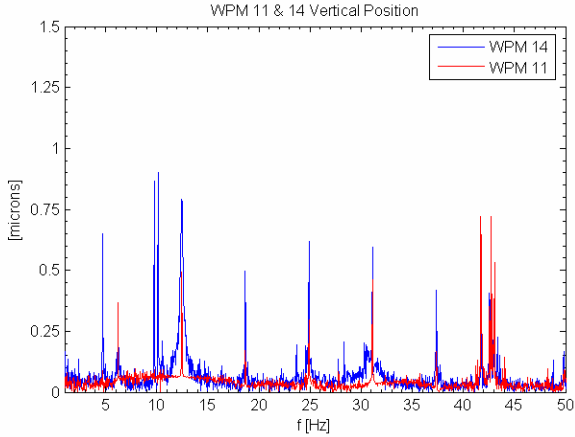

Figure 10: Spectra of cold mass vibrations in the vertical plane, detected by WPM # 11 and # 14

The operation of filtering the wire proper oscillations, though easy from the implementation point of view, is very delicate to perform, because often wire oscillation amplitudes can be up to a hundred of µm, against hundreds of nm maximum amplitude of microphonics. Often the microphonics signal is superimposed on wire oscillation spectral lines. So to avoid to cancel useful information, we have preferred not to filter completely the wire oscillation lines, stopping when microphonics signal is readable. Looking to the blue line spectra of WPM 14, a significant amount of noise is present between 10 Hz and 30 Hz, 30 Hz and 40 Hz, due to the proximity of vacuum pumps and similar devices, and under 10 Hz, possibly due to the cryogenic system. On the contrary, the spectra of the WPM 11 signals, which is at the central post position, show substantially only the harmonics (filtered) of the wire oscillations. In this case a clear indication of a signal around 44 Hz is visible and as well smaller signals at 27 Hz and 22 Hz. An asymmetry

between horizontal and vertical frequency is also presents. These effects will be the starting point for future investigations. The differences between the central and end positions noise magnitudes are less evident on cryomodule # 4 (WPMs # 4 and # 7), though spectral lines due to the pumping activity are still present on the monitor close to the cryomodule end. This situation is more evident comparing the power spectral densities (PSD), computed using equation (3).The graphs for the two cryomodules, are shown in Fig. 11 and Fig. 12.

$$PSD\left(\frac{n}{NT}\right) = \frac{\frac{1}{2}\left|G\left(\frac{n}{NT}\right)\right|^2}{df} \qquad (3)$$
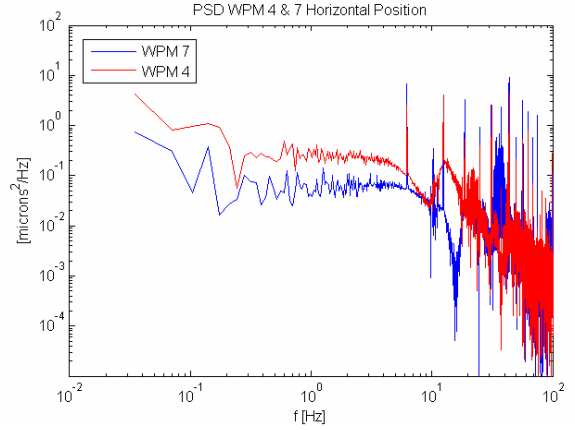
$$df = \frac{f_S}{N} = \frac{1}{T}$$

Figure 11: Power Spectral Density of the cold mass vibrations in the horizontal plane detected by WPM # 4 and # 7

Looking to Fig. 11, one can see that unexpected noise at very low frequency has been found on the signals coming from WPM # 4. Further tests must be done to understand if this is a real noise coming from the cold mass or it is a common mode interference (the WPM electronic system cabinet is very close to the klystrons!).
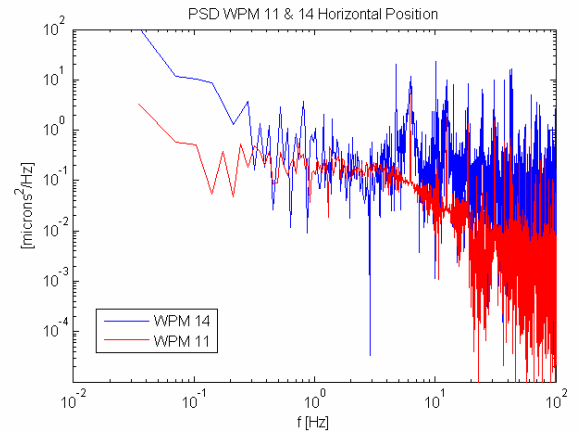

Figure 12: Power Spectral Density of the cold mass vibrations in the horizontal plane detected by WPM # 11 and # 14

To complete our analysis we have computed the integrated RMS value up to 100 Hz, of the vibration noise (the square root of the variance), using the following equation:

$$\sigma\left(\frac{n}{N\tau}\right) = \sqrt{df \cdot \sum_{l=n}^{\frac{N}{2}-1} PSD\left(\frac{l}{N\tau}\right)} \qquad (4)$$

The noise contribution coming from the first WPM in the monitor chain of each cryomodule has been inserted in the graphs, as shown in Fig. 13 and Fig. 14. WPM # 1 and # 8 are at the beginning of the cryomodule # 4 & # 5 respectively.
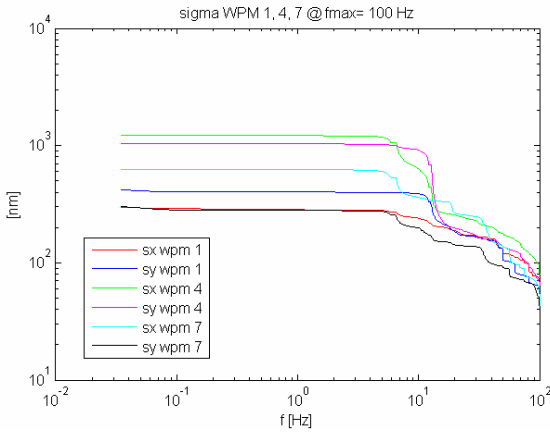

Figure 13: Microphonics noise RMS amplitude value @ f_{max}= 100 Hz for the cryomodule # 4

Observing the green and purple lines in Fig. 13, is evident that the variances of the noise coming from WPM # 4 is dominated by the low frequency contributions, as expected after the analysis of the PSD graph (Fig. 11). Moreover, for all the monitors, a small contribution to the RMS value comes from the spectral losses of the wire self oscillations lines. A more efficient procedure to remove these contributions when computing integrated RMS values is under study.
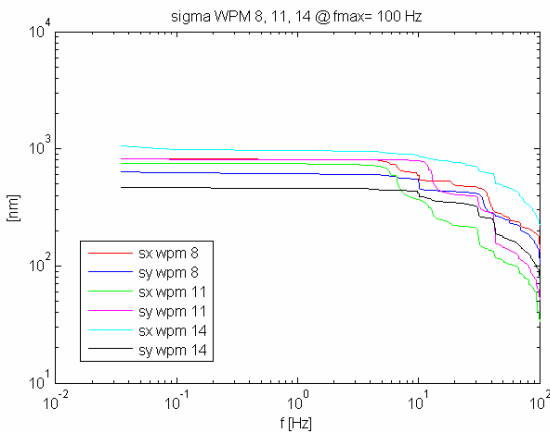

Figure 14: Microphonics noise RMS amplitude value @ f_{max}= 100 Hz for the cryomodule # 5

CONCLUSIONS

The WPM system has proved to be useful to detect low frequency mechanical vibrations, well below the 100 nm threshold. Higher efficiency and flexibility can be reached investing more resources in the optimization of the electronic system (e.g.: RF multiplexers and ad hoc AGC amplifier boards) which would completely make automatic the acquisition of all the vibration spectra needed. Additional work has to be done on the removal of the stretched wire proper oscillation, that up to now is the biggest problem towards nanometer resolution. Despite this drawback, the information retrieved up to now on cold mass microphonics noise are very useful for the study of the future ILC (and TTF) cryomodule assembling and for this purpose, can be cross-checked with the results of the traditional methods of low frequency vibration detection [6, 7].

REFERENCES

[1] A. Bosotti, C. Pagani, P. Pierini, R. Lange, R. De Monte and M. Ferianis, Analysis of the Cold Mass Displacements at the TTF, EPAC'04, Lucerne, July 2004, p. 1681.

[2] A. Bosotti, C. Pagani, R. Paparella, P. Pierini, R. Lange, R. De Monte and M. Ferianis, Mechanical Vibration Measurements on TTF Cryomodules,. PAC'05, Knoxville, May 2005, to be published.

[3] R. Ursic and R. De Monte,. Digital Receivers Offer New Solutions for Beam Instrumentation, PAC'99, New York, March-April 1999, p. 2253.

[4] Instrumentation Technologies, QDR, Technical Reference User Manual, November 12, 2002.

[5] J.W. Cooley, P.A.W. Lewis and P.D. Welch, The Finite Fourier Transform, IEEE Transactions On Audio And Electroacoustics, June 1969, Vol. AU-17 No. 2, p.77.

[6] H. Brueck, Vibration Measurements at TTF, TESLA Meeting, Hamburg March 31, 2005.

[7] W. Bialowons and H. Ehrlichmann, First Results of the Vibration Measurements with Seismic Sensors at TTF Modules, XFEL LINAC Module Meeting Hamburg, September 2, 2004.